arXiv:1511.05776v3 [physics.atom-ph] 11 Apr 2016

Importance of the completeness of the configuration interaction and close coupling expansions in R-matrix calculations for highly-charged ions: electron-impact excitation of Fe^{20+}

L Fernández-Menchero[1]‡, A S Giunta[2], G Del Zanna[3] and N R Badnell[1]

[1]Department of Physics, University of Strathclyde, Glasgow G4 0NG, UK
[2]STFC Rutherford Appleton Laboratory, Chilton, Didcot, Oxon. OX11 0QX, UK
[3]Department of Applied Mathematics and Theoretical Physics, University of Cambridge, Cambridge CB3 0WA, UK

Abstract.

We have carried-out two intermediate coupling frame transformation (ICFT) R-matrix calculations for the electron-impact excitation of C-like Fe^{20+}, both of which use the same expansions for their configuration interaction (CI) and close-coupling (CC) representations. The first expansion arises from the configurations $2s^2\,2p^2$, $2s\,2p^3$, $2p^4$, $\{2s^2\,2p$, $2s\,2p^2$, $2p^3\}\,nl$, with $n = 3, 4$, for $l = 0{-}3$, which give rise to 564 CI/CC levels. The second adds configurations $2s^2\,2p\,5l$, for $l = 0 - 2$, which give rise to 590 CI/CC levels in total.

Comparison of oscillator strengths and effective collision strengths from these two calculations demonstrates the lack of convergence in data for $n = 4$ from the smaller one. Comparison of results for the 564 CI/CC level calculation with an earlier ICFT R-matrix calculation which used the exact same CI expansion but truncated the CC expansion to only 200 levels demonstrates the lack of convergence of the earlier data, particularly for $n = 3$ levels. Also, we find that the results of our 590 CC R-matrix calculation are significantly and systematically larger than those of an earlier comparable Distorted Wave-plus-resonances calculation.

Thus, it is important still to take note of the (lack of) convergence in both atomic structural and collisional data, even in such a highly-charged ion as Fe^{20+}, and to treat resonances non-perturbatively. This is of particular importance for Fe ions given their importance in the spectroscopic diagnostic modelling of astrophysical plasmas.

PACS numbers: 34.50.Fa,52.20.Fs,95.30.Ky

Submitted to: *J. Phys. B: At. Mol. Phys.*

‡ Present address: Department of Physics and Astronomy, Drake University. Des Moines IA, 50311, USA

1. Introduction

Accurate data for Fe^{20+} are required for solar physics applications. The forbidden line of Fe XXI at 1354.1 Å is observed routinely with the Interface Region Imaging Spectrograph (IRIS [1]), launched in July 2013. IRIS has been producing excellent spectra and images of the solar atmosphere at very high resolution, and this line is used to study solar flares (see, e.g. [2, 3]).

The $n = 2 \rightarrow n = 2$ transitions in the soft X-rays are known to be excellent density diagnostics for solar flare plasma, as shown e.g. in [4, 5]. These lines have been observed routinely from 2010 until 2014 with the Extreme ultraviolet Variability Experiment (EVE) instrument on-board the Solar Dynamics Observatory (SDO). The resonance line, at 128.7 Å, during solar flares, becomes the dominant contribution to the 131 Å band of the SDO Atmospheric Imaging Assembly (AIA), as described in [6, 7]. Images from the AIA 131 Å band are routinely used since 2010 to study solar flares.

All of the iron ions have been studied during the course of the IRON project [8]. Several works exist for the electron-impact excitation of C-like Fe^{20+} spanning several decades. Bhatia *et al* [9] calculated energies and transition line strengths for the C-like ions from Ar^{12+} up to Kr^{30+}. Zhang and Sampson [10] calculated collision strengths with a distorted wave method for all the C-like ions from F^{3+} up to Xe^{48+}. They calculated all of the transitions within the $n = 2$ levels. Aggarwal [11] used the Dirac-Fock R-matrix method including in the configuration interaction (CI) and close coupling (CC) expansions all the configurations of $n = 2$, which leads to a total of 20 fine-structure levels. Aggarwal and Keenan [12] later improved upon their work by using a more extended basis set, now including some configurations of $n = 3$, for a total of 46 levels.

The previous work of Badnell and Griffin [13] used the Intermediate Coupling Frame Transformation (ICFT) R-matrix method [14]. The atomic structure was quite accurate, including in the CI expansion all of the configurations up to $n = 4$, obtaining a total of 564 levels. In the CC calculation only 200 levels were included of these 564 from the CI calculation. However, these 200 levels did not correspond to the lowest energetic ones. The goal of that work was to look at the effect of resonances attached to $n = 4$ levels on transitions from the ground configuration. To that end, the CC expansion included all $2s^2\,2p\,4l$ configurations but omitted the $2p^3\,3l$ (as well as all other $n = 4$ ones.) The argument being that the omitted ones (especially $n = 3$) could only couple weakly with the ground configuration. Computationally, it is now possible to investigate this.

The most recent work on Fe^{20+} appears to be that of Landi and Gu [15]§ who used a Distorted Wave (DW) method which took account of resonances attached to the $n = 2$ levels and the most important $n = 3$ levels, in the independent processes and isolated resonance approximations. Their CI expansion was a little larger, including three configurations with $n = 5$, for a total of 590 levels. Landi and Gu calculated collision strengths and effective collision strengths for electron-impact excitation from the ground and first two excited levels

§ Online material: `http://iopscience.iop.org/article/10.1086/500286/fulltext/tables.tar.gz`

of Fe^{20+}.

In present work we first include the 564 levels of Badnell and Griffin [13] in the CI & CC calculations. We use exactly the same atomic structure as in [13] so that we can study purely the completeness of the CC expansion. The effect of the completeness of the CI and CC expansions was studied in detail in [16]. In consequence we expect changes in the results of the effective collision strengths, mostly for transitions to the levels close to the cut-off of the basis set in [13]. The main effect should be due to additional resonance enhancement, which affects most strongly the weakest (forbidden) transitions at low temperatures ($< 10^6$ K).

In addition, we extend our calculation to use the same configuration expansion as Landi and Gu [15], by including the $2s^2\,2p\,5l$ with $l = 0 - 2$, for a total of 590 CI & CC levels. The addition of those 26 levels will improve the convergence of the expansion, mostly for the levels $2s^2\,2p\,4l$ with $l = 0 - 2$.

Finally, Fe^{20+} DW data were calculated with the AUTOSTRUCTURE program [17] as part of the baseline data improvement initiative for fusion within the EU FP7 programme‖ and the results were made available via the OPEN-ADAS database¶. The target CI expansion used the same set of configurations as the present one and [13], i.e. 564 levels, but the atomic structure was not optimized. Here we check the validity of these results by comparing them with the (DW) ones we obtain using the optimized target of [13]. We also look at the effect of unitarization on these DW results.

The paper is organised as follows. In section 2 we give details of the description of the atomic structure and in section 3 that of our *R*-matrix and distorted wave calculations. In section 4 we show some representative results and compare them with the results of the *R*-matrix calculations by [13] and with distorted wave ones. The main conclusions are presented in section 5.

The atomic data will be made available at our APAP network web page[+]. They will also be uploaded online in the CHIANTI atomic database[*] [18] and the Atomic Data and Analysis Structure one (OPEN-ADAS).

This work is part of the UK APAP Network and provides a template for treating the C-like isoelectronic sequences to follow our previous work on the Be-like [19], Mg-like [20], F-like [21], Ne-like [22], Li-like [23] and B-like [24].

Atomic units are used unless otherwise specified.

2. Structure

We want to compare results for two different CC expansions. To do so unambiguously we must keep the atomic structure exactly the same, as in [13]. Badnell and Griffin [13] used the AUTOSTRUCTURE program [17]. AUTOSTRUCTURE carries-out a diagonalization of the Breit–Pauli Hamiltonian [25] to obtain the eigenstates and energies of the target. Relativistic terms, viz.

‖ http://adas-eu.ac.uk
¶ http://open.adas.ac.uk
[+] http://www.apap-network.org
[*] http://www.chiantidatabase.org

mass-velocity, spin-orbit, and Darwin, are included as a perturbation. The multi-electron electrostatic interactions are described by a Thomas-Fermi-Dirac-Amaldi model potential with scaling parameters $\lambda_{\rm nl}$. In Badnell and Griffin [13] the $\lambda_{\rm nl}$ were determined through a variational method in which the equally-weighted sum of the energies of all the terms was minimized. In the present work we repeat the structure calculations with the same scaling parameters, but make new comparisons. We note that a non-optimized structure corresponds to setting all scaling parameters to unity.

The calculation of Badnell and Griffin [13] included a total of 10 atomic orbitals in the basis set: 1s, 2s, 2p, 3s, 3p, 3d, 4s, 4p, 4d, 4f. In the configuration interaction expansion are included all the configurations $\{(1s^2)\}$ $2s^2\,2p^2$, $2s\,2p^3$, $2p^4$, $2s^2\,2p\,nl$, $2s\,2p^2\,nl$, $2p^3\,nl$ for all nl orbitals previously mentioned with $n = 3, 4$, for a total of 24 configurations. The configuration list detailed above gives rise to a total of 268 LS terms, which on recoupling to take account of the spin-orbit interaction, give rise to 564 levels. We have performed a new calculation including three additional orbitals 5s, 5p, 5d. In addition to the configurations for the previous calculation, we included the $2s^2\,2p\,5l$ with $l = 0 - 2$. This new configuration list rises to a total of 282 LS terms and 590 IC levels. This is the same configuration list that was used by Landi and Gu [15], which is the most complete to-date. The minimized values of the scaling parameters for the present and previous work [13] are 1s 1.37988; 2s 1.25035; 2p 1.18359; 3s 1.38480; 3p 1.25830; 3d 1.39690; 4s 1.32721; 4p 1.25440; 4d 1.37130; 4f 1.44540. For present 590-level calculation, the scaling parameters for the three added orbitals are 5s 1.76478; 5p 1.41353; 5d 1.45655.

In table 1, we show the present intermediate coupling (IC) energies and compare them with the ones obtained by Badnell and Griffin [13], Landi and Gu [15], and the observed ones tabulated in the CHIANTI database; all for the 50 lowest target levels. The rest of the calculated level energies can be found online. The experimental data collected for CHIANTI contain data from the works of [26, 27, 28, 29, 30, 31] The agreement of the present energies with the observed values is within 1.5%, with a few exceptions in the lower excited singlet levels, and the relative errors are smaller in the present work than in previous theoretical ones with smaller basis sets, and more or less equal to the ones of [15] with the same configuration set. In some cases the lifetimes differ a larger quantity between the different atomic structures. For example in the case of 50th level it is more than a factor 2. This discrepancy is due to the level mixing, level 50 mixing is $2s\,2p^2\,3p\,{}^5D^o_0$ (75%), plus $2s^2\,2p\,3d\,{}^3P^o_0$ (17%), plus $2s\,2p^2\,3p\,{}^3P^o_0$ (5%). There is a part of 22% which connects with the ground state in an intense dipole transition, while the 75% correspond to a forbidden spin-change one. A slight change in the mixing of the least weight part will produce a large change in the life time, but not so in the energy.

To check the quality of the calculated wave functions of the target we compare the oscillator strengths (gf values) for selected transitions from the ground state in Table 2 for Fe^{20+} with data from [15]. Data for more transitions from ground term and other transition types can be found in the online material. Very good agreement, within 5%, is found in general. However, the gf values for the transitions $1 - 54$: $2s^2\,2p^2\,{}^3P_0 - 2s\,2p^2\,3p\,{}^3S^o_1$ and $1 - 56$: $2s^2\,2p^2\,{}^3P_0 - 2s^2\,2p\,3d\,{}^1P^o_1$ differ substantially from the ones of [15]. This is due

Table 1. Fe^{20+} target level energies (cm^{-1}) and lifetimes (s).

i	Conf.	Level	$E_{\rm CHIANTI}$	$E_{\rm th}$ (%)	$E_{\rm B01}$ (%)	$E_{\rm L06}$ (%)	$\tau_{\rm th}$	$\tau_{\rm B01}$	$\tau_{\rm L06}$
1	$2s^2\,2p^2$	$^3P_0$	0	0 (0.0)	0 (0.0)	0 (0.0)	–	–	–
2	$2s^2\,2p^2$	$^3P_1$	73851	72710 (1.5)	72595 (1.7)	73041 (1.1)	1.60 [−4]	1.61 [−4]	1.53 [−4]
3	$2s^2\,2p^2$	$^3P_2$	117367	119427 (1.8)	119252 (1.6)	117147 (0.2)	9.41 [−4]	9.45 [−4]	1.17 [−3]
4	$2s^2\,2p^2$	$^1D_2$	244568	246885 (0.9)	246568 (0.8)	245710 (0.5)	3.26 [−5]	3.28 [−5]	3.33 [−5]
5	$2s^2\,2p^2$	$^1S_0$	371744	372374 (0.2)	371983 (0.1)	373060 (0.4)	7.39 [−6]	7.42 [−6]	7.50 [−6]
6	$2s\,2p^3$	$^5S^o_2$	486991	478047 (1.8)	477618 (1.9)	479659 (1.5)	1.56 [−8]	1.56 [−8]	1.49 [−8]
7	$2s\,2p^3$	$^3D^o_1$	776685	776317 (0.0)	776093 (0.1)	779724 (0.4)	7.81 [−11]	7.80 [−11]	7.83 [−11]
8	$2s\,2p^3$	$^3D^o_2$	777367	777486 (0.0)	777258 (0.0)	779963 (0.3)	1.05 [−10]	1.04 [−10]	1.06 [−10]
9	$2s\,2p^3$	$^3D^o_3$	803553	806858 (0.4)	806644 (0.4)	805768 (0.3)	1.37 [−10]	1.36 [−10]	1.39 [−10]
10	$2s\,2p^3$	$^3P^o_0$	916333	915712 (0.1)	915430 (0.1)	920272 (0.4)	4.43 [−11]	4.42 [−11]	4.44 [−11]
11	$2s\,2p^3$	$^3P^o_1$	924920	925643 (0.1)	925364 (0.0)	928822 (0.4)	4.17 [−11]	4.17 [−11]	4.21 [−11]
12	$2s\,2p^3$	$^3P^o_2$	942364	944477 (0.2)	944210 (0.2)	946135 (0.4)	4.69 [−11]	4.69 [−11]	4.71 [−11]
13	$2s\,2p^3$	$^3S^o_1$	1095679	1101047 (0.5)	1100644 (0.5)	1105579 (0.9)	1.00 [−11]	1.00 [−11]	1.02 [−11]
14	$2s\,2p^3$	$^1D^o_2$	1127250	1135203 (0.7)	1134994 (0.7)	1137533 (0.9)	1.81 [−11]	1.81 [−11]	1.85 [−11]
15	$2s\,2p^3$	$^1P^o_1$	1260902	1268682 (0.6)	1268380 (0.6)	1272627 (0.9)	1.09 [−11]	1.09 [−11]	1.12 [−11]
16	$2p^4$	$^3P_2$	1646409	1652564 (0.4)	1652131 (0.3)	1657412 (0.7)	1.59 [−11]	1.59 [−11]	1.62 [−11]
17	$2p^4$	$^3P_0$	1735715	1740540 (0.3)	1740111 (0.3)	1747301 (0.7)	1.37 [−11]	1.37 [−11]	1.39 [−11]
18	$2p^4$	$^3P_1$	1740453	1744624 (0.2)	1744193 (0.2)	1750849 (0.6)	1.37 [−11]	1.37 [−11]	1.39 [−11]
19	$2p^4$	$^1D_2$	1817041	1828341 (0.6)	1827909 (0.6)	1832103 (0.8)	2.08 [−11]	2.08 [−11]	2.12 [−11]
20	$2p^4$	$^1S_0$	2048056	2060298 (0.6)	2059866 (0.6)	2066463 (0.9)	1.13 [−11]	1.13 [−11]	1.15 [−11]
21	$2s^2\,2p\,3s$	$^3P^o_0$	–	7694475 (–)	7694446 (–)	7654119 (–)	4.85 [−13]	4.92 [−13]	4.79 [−13]
22	$2s^2\,2p\,3s$	$^3P^o_1$	7661883	7704253 (0.6)	7704188 (0.6)	7663398 (0.0)	4.16 [−13]	4.22 [−13]	4.06 [−13]
23	$2s^2\,2p\,3s$	$^3P^o_2$	–	7805076 (–)	7805048 (–)	7770896 (–)	4.61 [−13]	4.68 [−13]	4.46 [−13]
24	$2s^2\,2p\,3s$	$^1P^o_1$	–	7831672 (–)	7831515 (–)	7796398 (–)	3.05 [−13]	3.09 [−13]	3.00 [−13]
25	$2s^2\,2p\,3p$	$^3D_1$	–	7873397 (–)	7873586 (–)	7834848 (–)	2.01 [−11]	1.91 [−11]	1.91 [−11]
26	$2s^2\,2p\,3p$	$^1P_1$	–	7930234 (–)	7930044 (–)	7891979 (–)	6.05 [−12]	5.78 [−12]	5.98 [−12]
27	$2s^2\,2p\,3p$	$^3D_2$	–	7933613 (–)	7933498 (–)	7895497 (–)	1.40 [−11]	1.34 [−11]	1.33 [−11]
28	$2s^2\,2p\,3p$	$^3P_0$	7915463	7950515 (0.4)	7950219 (0.4)	7909434 (0.1)	2.89 [−12]	2.72 [−12]	3.11 [−12]
29	$2s^2\,2p\,3p$	$^3P_1$	–	8010613 (–)	8010478 (–)	7977012 (–)	4.17 [−12]	4.05 [−12]	4.48 [−12]
30	$2s^2\,2p\,3p$	$^3D_3$	–	8020317 (–)	8020172 (–)	7987319 (–)	1.82 [−11]	1.74 [−11]	1.67 [−11]
31	$2s^2\,2p\,3p$	$^3S_1$	–	8031268 (–)	8031093 (–)	7998341 (–)	4.65 [−12]	4.46 [−12]	4.91 [−12]
32	$2s^2\,2p\,3p$	$^3P_2$	–	8037310 (–)	8037052 (–)	8002052 (–)	3.36 [−12]	3.25 [−12]	3.69 [−12]
33	$2s\,2p^2\,3s$	$^5P_1$	–	8101293 (–)	8100865 (–)	8070806 (–)	5.47 [−12]	6.54 [−13]	5.52 [−13]
34	$2s^2\,2p\,3p$	$^1D_2$	–	8101297 (–)	8100884 (–)	8065382 (–)	6.53 [−13]	5.32 [−12]	6.44 [−12]
35	$2s^2\,2p\,3d$	$^3F^o_2$	8074160	8114457 (0.5)	8114269 (0.5)	8072912 (0.0)	4.21 [−13]	4.22 [−13]	4.10 [−13]
36	$2s\,2p^2\,3s$	$^5P_2$	–	8149606 (–)	8149172 (–)	8121259 (–)	6.35 [−13]	6.35 [−13]	6.16 [−14]
37	$2s^2\,2p\,3d$	$^3F^o_3$	8118008	8153237 (0.4)	8152995 (0.4)	8111336 (0.1)	1.75 [−13]	1.74 [−13]	1.59 [−13]
38	$2s^2\,2p\,3d$	$^3D^o_2$	8124085	8160595 (0.4)	8160231 (0.5)	8118025 (0.1)	7.08 [−14]	7.08 [−14]	6.93 [−13]
39	$2s^2\,2p\,3p$	$^1S_0$	8143710	8162776 (0.2)	8162508 (0.2)	8126193 (0.2)	1.50 [−12]	1.48 [−12]	1.40 [−12]
40	$2s^2\,2p\,3d$	$^3D^o_1$	8141785	8179034 (0.5)	8178623 (0.5)	8135992 (0.1)	4.38 [−14]	4.38 [−14]	4.35 [−14]
41	$2s\,2p^2\,3s$	$^5P_3$	–	8199750 (–)	8199316 (–)	8170876 (–)	5.80 [−13]	5.80 [−13]	5.57 [−13]
42	$2s\,2p^2\,3s$	$^3P_0$	8180254	8216612 (0.4)	8216280 (0.4)	8179293 (0.0)	5.02 [−13]	5.04 [−13]	4.71 [−13]
43	$2s^2\,2p\,3d$	$^3F^o_4$	–	8232560 (–)	8232334 (–)	8195771 (–)	6.82 [−10]	6.78 [−10]	6.62 [−10]
44	$2s^2\,2p\,3d$	$^1D^o_2$	–	8240685 (–)	8240369 (–)	8204330 (–)	7.76 [−14]	7.79 [−14]	7.97 [−14]
45	$2s\,2p^2\,3s$	$^3P_1$	–	8252207 (–)	8251886 (–)	8217390 (–)	3.92 [−13]	3.93 [−13]	3.66 [−13]
46	$2s^2\,2p\,3d$	$^3D^o_3$	8229642	8264432 (0.4)	8264055 (0.4)	8227144 (0.0)	4.77 [−14]	4.78 [−14]	4.84 [−14]
47	$2s^2\,2p\,3d$	$^3P^o_0$	–	8276802 (–)	8276404 (–)	8243034 (–)	7.83 [−14]	7.86 [−14]	7.20 [−14]
48	$2s^2\,2p\,3d$	$^3P^o_1$	–	8276891 (–)	8276489 (–)	8241557 (–)	6.05 [−14]	6.07 [−14]	5.87 [−14]
49	$2s^2\,2p\,3d$	$^3P^o_2$	8229642	8278152 (0.6)	8277744 (0.6)	8241437 (0.1)	5.45 [−14]	5.46 [−14]	5.41 [−14]
50	$2s\,2p^2\,3p$	$^5D^o_0$	–	8289029 (–)	8288610 (–)	8259742 (–)	6.34 [−13]	6.30 [−13]	1.58 [−12]

i: level index; Conf.: configuration; Level: term/level designation (largest weight); $E_{\rm CHIANTI}$: observed energy from the CHIANTI database; $E_{\rm th}$: theoretical level energy, present work with 590-level CI expansion; $E_{\rm B01}$: previous work theoretical level energy [13]; $E_{\rm L06}$: previous work theoretical level energy [15]; %: percentage difference between theoretical and observed data; $\tau_{\rm th}$: lifetimes present work; $\tau_{\rm B01}$: lifetimes work [13]; $\tau_{\rm L06}$: lifetimes work [15]. $A[B]$ denotes $A \times 10^B$.

Table 2. Comparison of gf values for selected transitions of the ion Fe^{20+}. $A\,[B]$ denotes $A \times 10^B$.

gf values: dipole transitions			
Transition	Present work	ref [13]	ref [15]
1 – 7	8.730 [−2]	8.749 [−2]	8.629 [−2]
1 – 11	2.319 [−2]	2.317 [−2]	2.273 [−2]
1 – 13	3.642 [−2]	3.638 [−2]	3.563 [−2]
1 – 15	7.903 [−5]	7.730 [−5]	6.596 [−5]
1 – 22	5.141 [−2]	5.039 [−2]	5.435 [−2]
1 – 24	9.731 [−4]	9.735 [−4]	1.119 [−3]
1 – 40	1.286 [0]	1.284 [0]	1.307 [0]
1 – 48	5.630 [−3]	5.654 [−3]	4.090 [−3]
1 – 51	2.150 [−2]	2.150 [−2]	2.665 [−2]
1 – 54	4.267 [−2]	4.276 [−2]	1.742 [−2]
1 – 56	2.689 [−3]	2.588 [−3]	3.482 [−2]
1 – 58	1.887 [−1]	1.886 [−1]	1.995 [−1]
1 – 60	1.342 [−1]	1.342 [−1]	1.173 [−1]
1 – 70	3.480 [−2]	3.480 [−2]	3.378 [−2]
1 – 94	3.168 [−2]	3.176 [−2]	2.921 [−2]

to the large term mixing of the upper states: level 54 has a mixing of $2s\,2p^2\,3p\,{}^3S^o_1$ (42%), $2s\,2p^2\,3p\,{}^5D^o_1$ (35%) and $2s\,2p^2\,3p\,{}^5P^o_1$ (14%), and 56 has a mixing of $2s^2\,2p\,3d,{}^1\,P^o_1$ (77%), $2s^2\,2p\,3d,{}^3\,D^o_1$ (8%) and $2s^2\,2p\,3d,{}^3\,P^o_1$ (5%). Both levels mix strong dipole allowed transitions with forbidden spin-change ones. The case of transition 1 – 56 mixes a 77% of forbidden transition with just a 13% of dipole allowed one, so its sensitivity to the level mixing will be quite large, and because of that the value can differ by an order of magnitude with the one of Landi and Gu [15]. We find that a small variation of our scaling parameters can change the value of gf for these transitions by a factor of two.

We have made a similar comparison for infinite energy Plane-Wave Born limits, with Badnell and Griffin [13] only since Landi and Gu [15] do not provide them. We find a very similar pattern of agreement (not shown) to that shown in Table 2 for gf-values.

In fig. 1 we show a diagram comparing the gf values for the atomic structures of the works [13] and [15] for the transitions between all the levels. For transitions between levels of $n = 2$ all the points spread less than a 10% from the (diagonal) line of equality. This demonstrates that the CI expansion is sufficiently converged for the $n = 2$ states as both lead to essentially the same results. For transitions involving states of $n = 3$ the dispersion is larger. We find some points in which both calculations differ several orders of magnitude. Nevertheless, most of them differ less than a factor 2. For $n = 4$ the dispersion is quite large, with many points far away of the line of equality. This is a consequence of the expansion not being converged for the highest excited states. This result is to be expected, following the work by [16]. In fig. 2 we show the same comparison for the structure of the present 590-

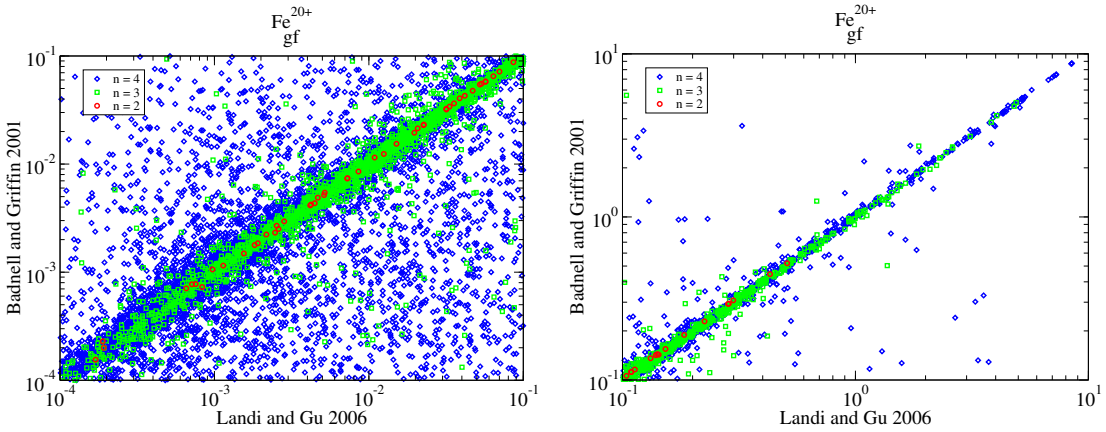

Figure 1. Comparison of gf for the two atomic structures of works of Badnell and Griffin [13] and Landi and Gu [15], 564- vs 590-level CI expansions of Fe^{20+}. ○: transitions with upper level with $n = 2$; □: transitions with upper level with $n = 3$; ⋄: transitions with upper level with $n = 4$. Left panel: weak transitions ($gf < 0.1$); Right panel: strong transitions ($gf > 0.1$). Colour online.

level calculation with the one of [15]. This time both structures use the same CI expansion, although the orbitals themselves differ. The dispersion is much smaller than in the previous figure. The convergence for the levels $2s^2\,2p\,4l$ with $l = 0 - 2$ has improved considerably. The 26 new levels included will not increase the computation time by a large amount, but the quality of the atomic structure of the target is better now. Levels have a large mixing between configurations of $n = 4$ and $n = 5$, so the configuration can not be identified as a good quantum number for the highest excited levels. In table 3 we give the exact number of transitions which have an error larger than a certain threshold in figs. 1 and 2.

In fig. 3 we restrict the comparison of the gf factors to the transitions from the ground level. The levels of $n = 3$ which lie far from the diagonal are states with large term mixing between forbiden and dipole allowed transitions. For these levels the oscillator strengths are quite sensitive to the mixing. We see that when restricted to the ground level the data for $n = 4$ are as well converged as for $n = 3$. Transitions from the other levels of the ground term are also important for astrophysical application and we obtain a very similar pattern of agreement (not shown) as to the ground level.

3. Scattering

For the scattering calculation, we use the same method as in [13]. It consists of an R-matrix formalism [8, 32] combined with an intermediate coupling frame transformation (see [13, 33]) to include the spin-orbit mixing efficiently and accurately. The accuracy of the method, compared to a full Breit-Pauli R-matrix (BPRM) calculation has been studied most recently in [16]. The differences between the ICFT and BPRM methodologies are swamped by the uncertainties and inaccuracies due to the use of truncated CI and CC expansions.

In the R-matrix formalism, the configuration space is divided in two regions: inner and

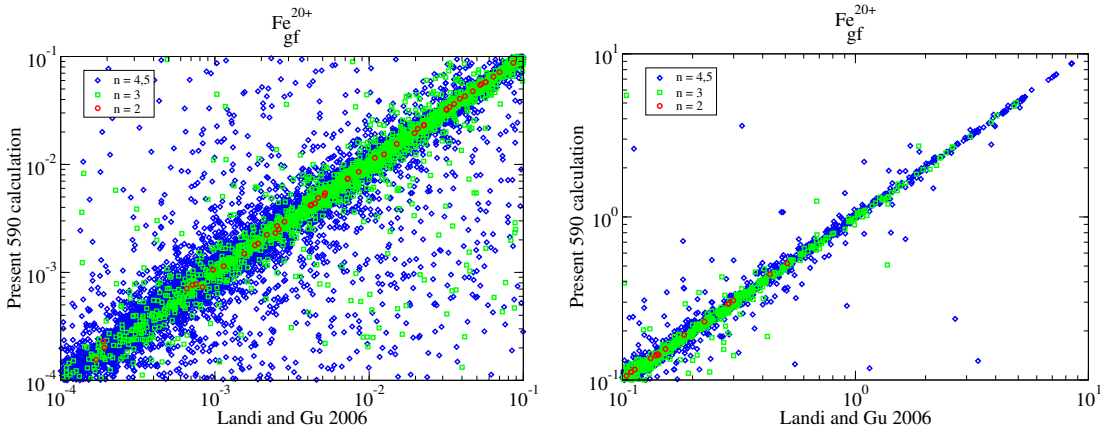

Figure 2. Comparison of gf for the two atomic structures of works of Landi and Gu [15] 590-level with AUTOSTRUCTURE one with the same CI expansion of Fe^{20+}. ○: transitions with upper level with $n = 2$; □: transitions with upper level with $n = 3$; ⋄: transitions with upper level with $n = 4$. ▽: transitions with upper level with $n = 5$. Left panel: weak transitions ($gf < 0.1$); Right panel: strong transitions ($gf > 0.1$). Colour online.

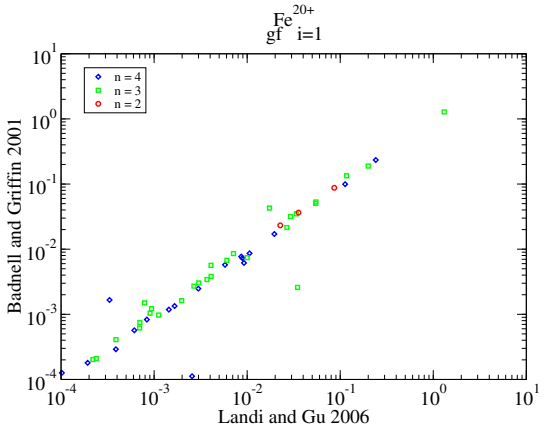

Figure 3. Same as figure 1, restricting to lower level the ground one. ○: transitions with upper level with $n = 2$; □: transitions with upper level with $n = 3$; ⋄: transitions with upper level with $n = 4$. Colour online.

outer. In this calculation we also split the inner region calculation in two parts: exchange and non-exchange. In the part including the electron exchange effects we included angular momenta up to $2J = 23$. In the part that we neglected the exchange effects, we increased the maximum angular momentum to $2J = 77$. To get higher angular momenta, up to infinity, we used the top-up formula of the Burgess sum rule [34] for dipole allowed transitions, and a geometric series for the remaining Born allowed transitions (see [13]). We set the number of continuum basis orbitals per angular momentum to 40, the smallest highest orbital energy is 1400 Ry. The largest total number of channels obtained is 2870 for the calculation with 564 levels, and 2978 for the one with 590 levels.

In the outer region, we also split the calculation in two parts. In a low energy part, for impact energies up to the last excited level calculated, we used a fine energy mesh step of

Table 3. Number of transitions in Figs 1 and 2 which differ by more than a certain relative error $\delta = |gf - gf_{\rm LG}|/gf_{\rm LG}$ as a percentage.

Rel. error (%)	564 [13] vs 590 [15]	590 AS vs 590 [15]
Strong transitions ($gf > 0.1$)		
10	506	389
20	396	225
50	326	135
100	280	104
200	247	75
500	221	70
1000	187	66
Weak transitions ($gf < 0.1$)		
10	8192	6848
20	6371	4214
50	4647	2001
100	850	442
200	617	222
500	400	121
1000	267	86
Total	13816	14887

approximately $3.46 \times 10^{-6} z^2$ Ry, with $z = 20$, the charge of the ion, to resolve the resonances sufficiently. We extended the high energy part from the last excitation threshold to three times the ionization potential. In this region the collision strengths vary smoothly, so we used a coarse mesh of $1.61 \times 10^{-4} z^2$ Ry. For energies above the last calculated one, we used the infinite energy limit Plane-Wave Born $\Omega^{\infty}_{\rm PWB}$ and dipole line strengths S from AUTOSTRUCTURE and interpolated in a Burgess-Tully diagram [35] for each type of transition.

To obtain the effective collision strengths Υ we convolute the collision strengths Ω with a Maxwell equilibrium distribution at an electron temperature T:

$$\Upsilon(i-j) \;=\; \int_0^\infty \exp\left(-\frac{E}{kT}\right) \Omega(i-j)\, \mathrm{d}\left(\frac{E}{kT}\right), \qquad (1)$$

where E is the final energy of the scattered electron, T the electron temperature and k the Boltzmann constant. We calculated the effective collision strengths for electron temperatures between 10^5 and 10^9 K. That range covers the interest for both astrophysical and fusion plasmas. Results are stored as a type 3 ADAS Atomic Data Format *adf04* file in the OPEN-ADAS database [36].

4. Results

We calculated the ordinary collision strengths Ω and Maxwell-averaged effective collision strengths Υ for the electron-impact excitation of the ion C-like Fe^{20+}. In the first calculation

using the structure of [13] we calculated the whole transition matrix with the *R*-matrix method, between the 564 fine structure levels arising in the $n = 2-4$ electronic shells, which makes for a total of 158 766 inelastic transitions. For the second calculation with the larger expansion, the 590 fine-structure levels give rise to a total of 173 755 inelastic transitions.

Firstly, we compare results of the previous work of Badnell and Griffin [13] with the ones we obtained with the same atomic structure but using the more complete close-coupling expansion. Then we compare the DW work of Landi and Gu [15] with our 564 CC and 590 CC level *R*-matrix calculations. Finally, we compare a series of 564-level DW calculations with the 564 CC level *R*-matrix one, in which we look at the effect of unitarization and the use of a non-optimized atomic structure in the former. The non-optimized DW work used the same CI expansion as the optimized but we set all the scaling parameters λ to unity. These non-optimized non-unitarized DW results were uploaded to the OPEN-ADAS database in 2012 for use in plasma modelling♯.

Fig. 4 shows a comparison between the Υ calculated for all the transitions by Badnell and Griffin [13] with the ones for the present 564-level work. Both works use exactly the same atomic structure, but different expansions in the close coupling calculations. The present work includes all the 564 levels in the CC, while [13] only include the 200 most relevant, in principle, to get the Υ for transitions to $n = 4$. We display an intermediate temperature near to the peak abundance one, a lower one, and a higher one. For weak transitions [13] underestimates the results increasingly at low temperatures, by up to a factor of ~ 100 at $T = 8 \times 10^5$ K for some of them. This is due to the resonance enhancement associated with the additional states in the present much larger CC expansion. The results of [13] show little resonant enhancement for these worst cases. For intense transitions the resonances contribute less to the effective collision strengths, so the underestimation disappears. At higher temperatures the maximum of the Maxwellian distribution moves outside the resonance region and the effect is smaller, but still large. The number of states included in the CC calculation affects the results by a large amount, even when they use exactly the same atomic structure. That is in agreement with work [16]. In table 4 we give the exact number of values which differ less than a certain relative error from the diagonal line of equality.

Fig. 5 shows the same comparison, this time restricting just for the transitions from the ground level. It is these transitions which [13] argued could be calculated with the reduced CC expansion. Even using this restricted set of transitions the differences can be large, up to a factor 10. It is notable that it is transitions involving $n = 3$ which are affected most. The largest differences lie in transitions with double electron jumps or forbidden ones. These differences can not be attributed to atomic structure (configuration mixing) as both calculations used exactly the same one. The differences lie in the completeness of the close-coupling expansion. The differences are also smaller as the temperature increases. This is expected, as both sets of Ω tend to the same infinite energy limits. Such a comparison for the astrophysically-relevant transitions from the other fine-structure levels of the ground term looks very similar.

♯ `http://open.adas.ac.uk/detail/adf04/cophps][c/dw/ic][fe20.dat`

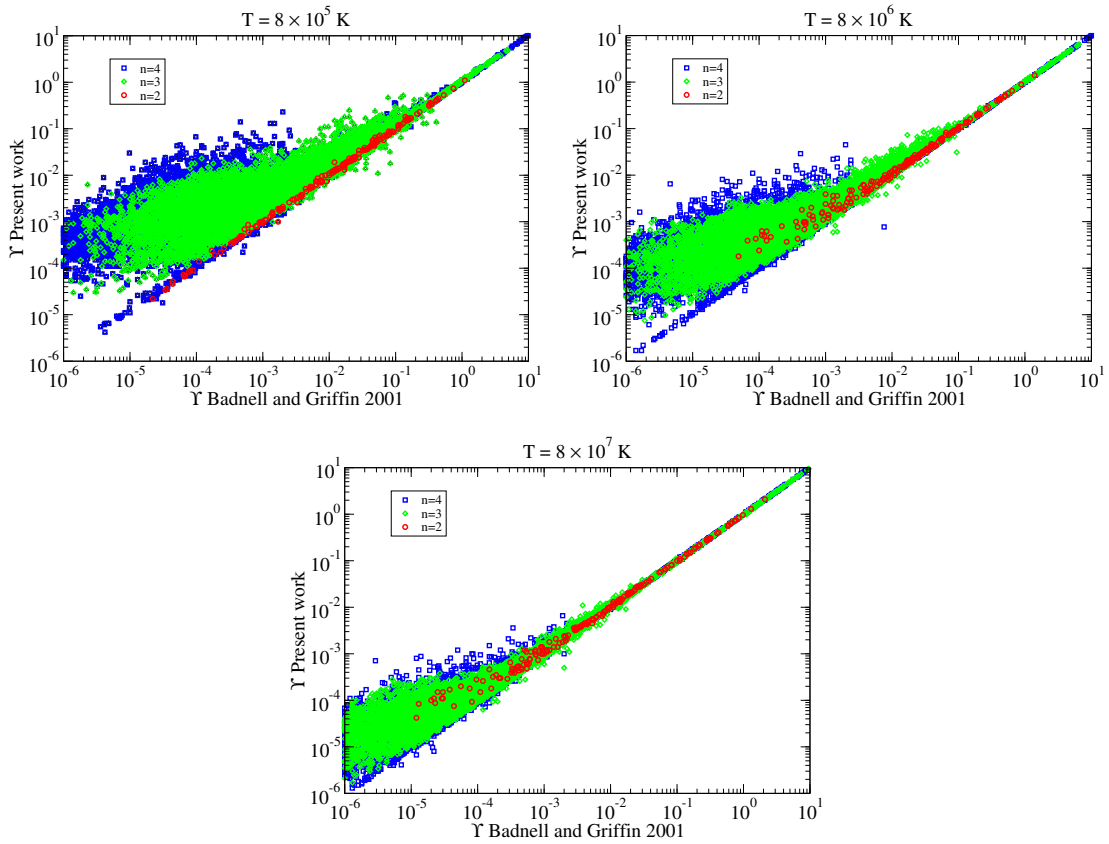

Figure 4. Comparison of the ϒ calculated with the two CC expansions for all the transitions. ∘: upper level up to $n = 2$. ⋄: upper level up to $n = 3$. □: upper level up to $n = 4$. Colour online.

Table 4. Number of transitions in Fig 4 which differ by more than a certain relative error $\delta = |\Upsilon_{200} - \Upsilon_{564}|/\Upsilon_{564}$ as a percentage.

Rel. error	Temperature (K)		
(%)	8×10^5	8×10^6	8×10^7
10	17931	15990	12375
20	16814	14775	10617
50	14872	12569	8274
100	13040	10520	6500
200	10772	8448	4946
500	8088	6186	3229
1000	6645	4684	2136
Total	19900	19900	19900

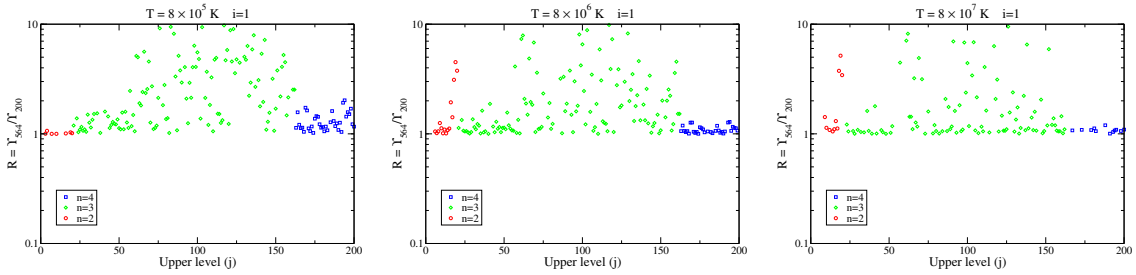

Figure 5. Ratio of the ϒ calculated with the two CC expansions (present and [13]) versus the upper level index from the ground level for three temperatures.

In fig. 6 we compare our *R*-matrix results for both CI/CC expansions with the 590-level DW ones of Landi and Gu [15]. The dispersion in the diagrams comparing the DW with the 564-level *R*-matrix calculation is much larger than that comparing with the 590-level *R*-matrix calculation. In addition, in the comparison with the 590-level *R*-matrix calculation there are very few points below the diagonal. The main differences between the 590-level calculations can be attributed to the additional resonance enhancement of the *R*-matrix calculation, while those with the 564-level one for levels with $n = 4$ are mainly related to atomic structure — compare with fig. 3. The additional 26 extra levels in the CI / CC expansions improves considerably the agreement of the collision data, as it did for the atomic structure, for the levels $2s^2\,2p\,4l$ with $l = 0 - 2$.

The differences between the DW+resonances results of Landi and Gu [15] and the 590-level *R*-matrix ones are due to differences in atomic structure and the difference between a perturbative and close-coupling treatment of resonances. Thus, we have performed a non-resonant unitarized DW calculation using the same atomic structure as the 590-level *R*-matrix one. Fig. 7 shows the comparison between both calculations *R*-matrix and UDW for the transitions tabulated in [15]. Now the only differences are due solely to the resonances, and strong coupling in general. Qualitatively, the dispersion in fig. 7 is comparable to that in fig. 6 and, indeed, quantitatively (see table 5) the level of disagreement between the two Distorted Wave calculations and *R*-matrix is very similar, despite one including resonances and the other not. We note an earlier small study on Mg-like ions [37], which compared *R*-matrix with DW-plus-resonances utilizing identical atomic structure, found significantly stronger resonance contributions from *R*-matrix due to interacting resonances, i.e. a breakdown of the isolated resonance approximation used by the perturbative DW approach.

Fig. 8 shows a comparison between several DW calculations. We show some selected transitions, the $5 - 20$: $2s^2 2p^2\ ^1S_0 - 2p^4\ ^1S_0$ one is an optically forbidden $J - J' = 0 - 0$ one dominated by coupling. It is the kind of transition which is sensitive to the unitarization of the DW method [38]. We also compare two atomic structures, the optimized one, as it is explained in section 2, and a simplified one, which has the same set of configurations, but all the scaling parameters λ_{nl} have been fixed to unity. The calculation of non-unitarized DW with the non-optimized atomic structure is the one available in the OPEN-ADAS database since 2012. DW calculations for both atomic structures agree to $\sim 1\%$. The UDW underestimates the collision

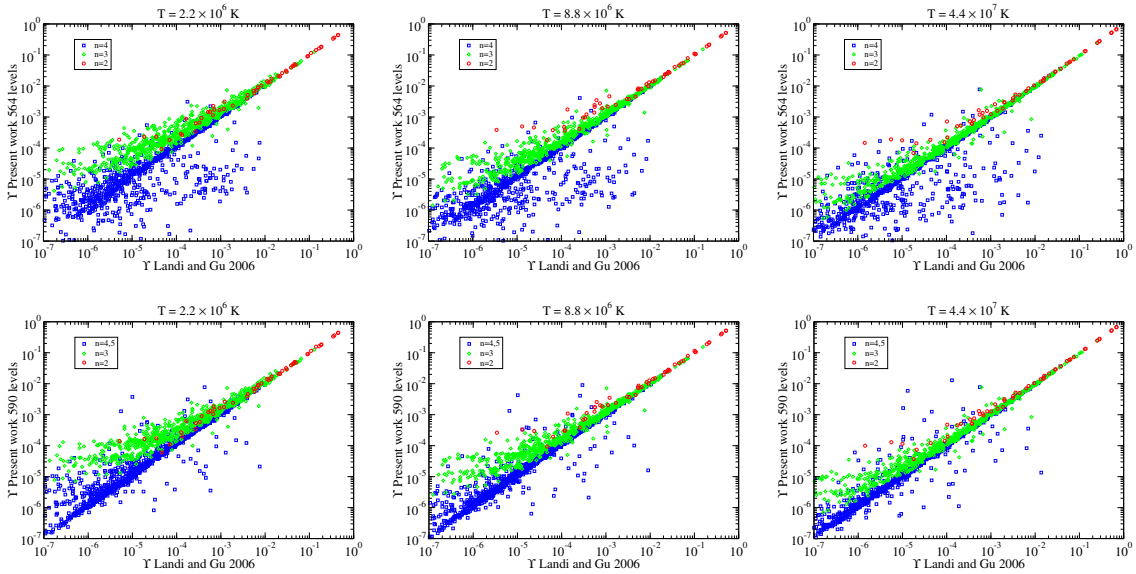

Figure 6. Comparison for the ϒ calculated in present work with the ones of Landi and Gu [15] from the three lowest levels for three temperatures and the two CI/CC expansions. Above diagrams, comparison with the 564-level *R*-matrix calculation; below diagrams, comparison with the 590-level *R*-matrix calculation.

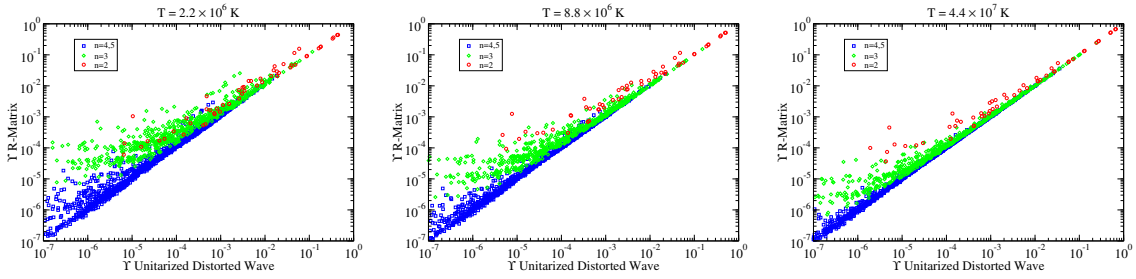

Figure 7. Comparison for the ϒ calculated in present work with the *R*-matrix and UDW methods with the same atomic structure of the target (590 levels) from the three lowest levels for three temperatures.

Table 5. Number of transitions in Figs 6 and 7 which differ by more than a certain relative error $\delta = |\Upsilon - \Upsilon_{\rm RM}|/\Upsilon_{\rm RM}$ as a percentage. $T = 8.8 \times 10^6$ K.

Rel. error (%)	RM vs DW+res [15]	RM vs UDW
10	1297	1127
20	1019	815
50	691	564
100	490	387
200	354	254
500	206	127
1000	124	71
Total	1764	1764

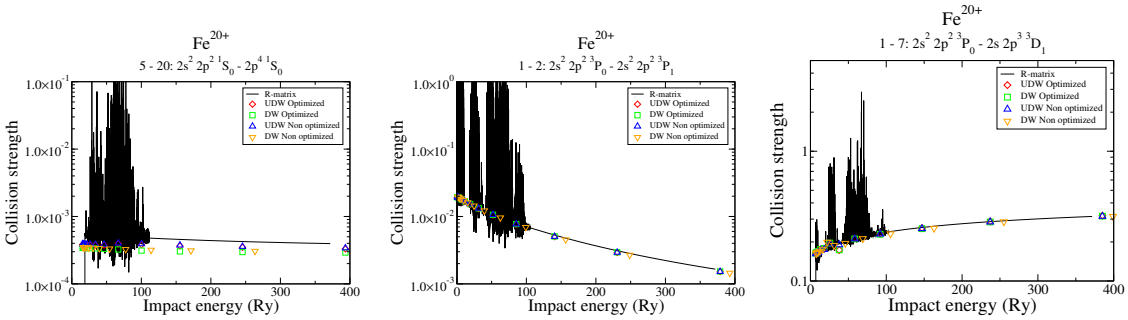

Figure 8. Comparison of the Ω calculated with different optimized atomic structures and unitarized and non-unitarized formalism. 564-level CI / CC expansions. Full line: *R*-matrix; ⋄: AS-UDW optimized atomic structure; □: AS-DW optimized atomic structure; △: AS-UDW simplified atomic structure; ▽: AS-DW simplified atomic structure; Colour online.

strength compared to the *R*-matrix one by ∼ 10%. The non-unitarized DW calculation gives rise to a larger underestimate, of 20%. The effects of the scaling parameter is small in the final results, as should perhaps be expected for such a relatively simple highly charged ion. Thus, the DW data archived in OPEN-ADAS are valid for plasma modelling when transitions are not strongly resonance enhanced.

As a sample of the best results obtained, the ones of the 590-level *R*-matrix calculation, fig. 9 shows the calculated effective collision strength compared with the previous works tabulated in CHIANTI database [13, 15] for some selected transitions. We show the intense electric dipole transition $1-7$, the forbidden M1 one which decays to the 1354.1 Å line $1-2$, the one-photon forbidden $J-J'=0-0$ one $1-10$. The rest of the values of the effective collision strengths for all of the 173 755 inelastic transitions can be found online.

For the electric dipole transition $1-7$, both CC expansions of the present work and [13] lead to the same results. The difference in the size of the CC expansions affects the resonance region, and for intense dipole transitions it is a small contribution. There is a difference between the *R*-matrix and the DW calculations for the optically forbidden transition $1-10$ $2s^2\,2p^2\,{}^3P_0 - 2s\,2p^3\,{}^3P_0$. This is due to the resonance contribution. Landi and Gu [15] used the the independent-processes and isolated-resonance approximations to include only resonances attached to the $n=2$ levels and some of the $n=3$, as discussed earlier. The DW and *R*-matrix calculations lead to the same results for dipole transitions. For the forbidden transition $1-10$ we appreciate a resonance enhancement with respect to the old calculation [13] at low temperature.

5. Conclusions

We have calculated a complete data set for the electron-impact excitation of the C-like ion Fe^{20+} using the ICFT *R*-matrix method. We have checked the effects in the final results of including some relevant configurations of $n=5$ in the CI expansion and the truncation of the CC expansion of the *R*-matrix calculation with respect to the CI expansion. Including just 26 $n=5$ levels in the CI / CC expansions does not increase substantially the computing resources

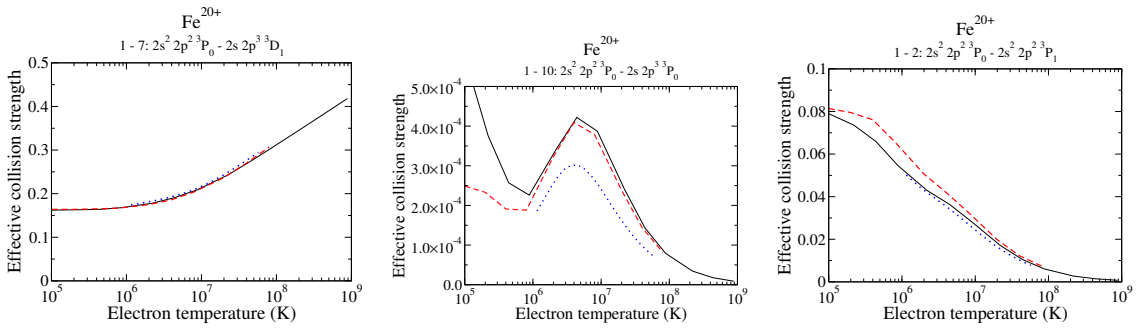
Fe20+
1 - 7: 2s2 2p2 3P0 - 2s 2p3 3D1
Effective collision strength
Electron temperature (K)
Fe20+
1 - 10: 2s2 2p2 3P0 - 2s 2p3 3P0
Effective collision strength
Electron temperature (K)
Fe20+
1 - 2: 2s2 2p2 3P0 - 2s2 2p2 3P1
Effective collision strength
Electron temperature (K)

Figure 9. Electron-impact excitation effective collision strengths versus the electron temperature for some selected transitions within the $n = 2$ complex. Full line: present work; dashed line: previous work [13]; dotted line: work [15]. Colour online.

required, but it improves significantly the convergence of the configuration interaction expansion of the target, for the levels $2s^2\,2p\,4l$ with $l = 0 - 2$. The truncated CC expansion of [13] underestimates substantially the results between excited states, but transitions from the ground configuration less so, mainly for the weak transitions and low temperatures. This is due to the coupling with states in the larger expansion which are not present in the smaller one.

The DW+resonances data of Landi and Gu [15] were to-date the most extensive and accurate calculation for the electron-impact excitation effective collision strengths of Fe^{20+} for transitions from the three lowest levels. The present calculation uses an atomic structure of the same quality as that of [15] and calculates the whole transition matrix with an *R*-matrix method. This full treatment of coupling and resonances gives rise to significant differences (increases, generally) compared to the results of Landi and Gu [15] while differences due to the remaining differences in atomic structure are likely (much) smaller.

We have also compared our DW results for an optimized atomic structure with an earlier non-optimized one. Results for both atomic structures are generally in good agreement. The optimization of the atomic structure does not affect significantly in the final results for such a highly-charged ion. In this sense, the DW data for Fe^{20+} present in OPEN-ADAS database since 2012 can be used for plasma modelling. However, we find significant differences between this DW data and the present *R*-matrix data due to the omission of resonances, and coupling more generally.

Even in Fe^{20+}, it is necessary to ensure that the CI and CC expansions are converged sufficiently. Thus, in the future, we plan apply this same *R*-matrix approach to C-like Ni^{22+} for astrophysical modelling applications.

Acknowledgments

The present work was funded by STFC (UK) through the University of Strathclyde UK APAP Network grant ST/J000892/1, the University of Cambridge DAMTP grant and the European Framework 7 ADAS-EU support action.

References

[1] De Pontieu B, Title A M, Lemen J R, Kushner G D, Akin D J, Allard B, Berger T, Boerner P, Cheung M, Chou C, Drake J F, Duncan D W, Freeland S, Heyman G F, Hoffman C, Hurlburt N E, Lindgren R W, Mathur D, Rehse R, Sabolish D, Seguin R, Schrijver C J, Tarbell T D, Wülser J P, Wolfson C J, Yanari C, Mudge J, Nguyen-Phuc N, Timmons R, van Bezooijen R, Weingrod I, Brookner R, Butcher G, Dougherty B, Eder J, Knagenhjelm V, Larsen S, Mansir D, Phan L, Boyle P, Cheimets P N, DeLuca E E, Golub L, Gates R, Hertz E, McKillop S, Park S, Perry T, Podgorski W A, Reeves K, Saar S, Testa P, Tian H, Weber M, Dunn C, Eccles S, Jaeggli S A, Kankelborg C C, Mashburn K, Pust N, Springer L, Carvalho R, Kleint L, Marmie J, Mazmanian E, Pereira T M D, Sawyer S, Strong J, Worden S P, Carlsson M, Hansteen V H, Leenaarts J, Wiesmann M, Aloise J, Chu K C, Bush R I, Scherrer P H, Brekke P, Martinez-Sykora J, Lites B W, McIntosh S W, Uitenbroek H, Okamoto T J, Gummin M A, Auker G, Jerram P, Pool P and Waltham N 2014 *Solar Physics* **289** 2733–2779 (*Preprint* 1401.2491)

[2] Young P R, Tian H and Jaeggli S 2015 *Astrophys. J.* **799** 218 (*Preprint* 1409.8603)

[3] Polito V, Reeves K K, Del Zanna G, Golub L and Mason H E 2015 *Astrophys. J.* **803** 84

[4] Mason H E, Bhatia A K, Neupert W M, Swartz M and Kastner S O 1984 *Solar Physics* **92** 199–216

[5] Del Zanna G and Woods T N 2013 *Astron. Astrophys.* **555** A59

[6] O'Dwyer B, Del Zanna G, Mason H E, Weber M A and Tripathi D 2010 *Astron. Astrophys.* **521** A21

[7] Petkaki P, Del Zanna G, Mason H E and Bradshaw S 2012 *Astron. Astrophys.* **547** A25

[8] Hummer D G, Berrington K A, Eissner W, Pradhan A K, Saraph H E and Tully J A 1993 *Astron. Astrophys.* **279** 298–309

[9] Bhatia A K, Seely J F and Feldman U 1987 *Atomic Data and Nuclear Data Tables* **36** 453

[10] Zhang H L and Sampson D H 1996 *Atomic Data and Nuclear Data Tables* **63** 275 – 314 ISSN 0092-640X/96

[11] Aggarwal K M 1991 *Astrophys. J. Suppl. Ser.* **77** 677–696

[12] Aggarwal K M and Keenan F P 1999 *J. Phys. B* **32** 3585

[13] Badnell N R and Griffin D C 2001 *J. Phys. B* **34** 681–697

[14] Griffin D C, Badnell N R and Pindzola M S 1998 *J. Phys. B* **31** 3713–3727

[15] Landi E and Gu M F 2006 *Astrophys. J.* **640** 1171–1179

[16] Fernández-Menchero L, Del Zanna G and Badnell N R 2015 *Mon. Not. R. Astr. Soc.* **450** 4174–4183

[17] Badnell N R 2011 *Comput. Phys. Commun.* **182** 1528–1535

[18] Landi E, Young P R, Dere K P, Del Zanna G and Mason H E 2013 *Astrophys. J.* **763** 86

[19] Fernández-Menchero L, Del Zanna G and Badnell N R 2014 *Astron. Astrophys.* **566** A104

[20] Fernández-Menchero L, Del Zanna G and Badnell N R 2014 *Astron. Astrophys.* **572** A115

[21] Witthoeft M C, Whiteford A D and Badnell N R 2007 *J. Phys. B: At. Mol. Opt. Phys.* **40** 2969–2993

[22] Liang G Y and Badnell N R 2010 *Astron. Astrophys.* **518** A64

[23] Liang G Y and Badnell N R 2011 *Astron. Astrophys.* **528** A69

[24] Liang G Y, Whiteford A D and Badnell N R 2009 *Astron. Astrophys.* **499** 943–954

[25] Eissner W M, Jones M and H N 1974 *Comput. Phys Commun.* **8** 270

[26] Feldman U, Curdt W, Landi E and Wilhelm K 2000 *The Astrophysical Journal* **544** 508 URL http://stacks.iop.org/0004-637X/544/i=1/a=508

[27] Martin W C, Fuhr J R, Kelleher D E, Musgrove A, Sugar J, Wiese W L, Mohr P J and Olsen K J 1999 *NIST Physical Reference Data* URL http://physics.nist.gov/asd

[28] Brown G V, Beiersdorfer P, Liedahl D A, Widmann K, Kahn S M and Clothiaux E J 2002 *The Astrophysical Journal Supplement Series* **140** 589 URL http://stacks.iop.org/0067-0049/140/i=2/a=589

[29] Fawcett B C, Jordan c, Lemen J and Phillips K 1987 *Monthly Notices of the Royal Astronomical Society* **225** 1013–1023

[30] Landi E and Phillips K J H 2005 *The Astrophysical Journal Supplement Series* **160** 286 URL http://stacks.iop.org/0067-0049/160/i=1/a=286

[31] P Palmeri, C Mendoza, T R Kallman and M A Bautista 2003 *Astron. Astrophys.* **403** 1175–1184

[32] Berrington K A, Eissner W B and Norrington P H 1995 *Comput. Phys. Commun.* **92** 290

[33] Badnell N R, Griffin D C and Mitnik D M 2001 *Journal of Physics B: Atomic, Molecular and Optical Physics* **34** 5071 URL http://stacks.iop.org/0953-4075/34/i=24/a=309

[34] Burgess A 1974 *Journal of Physics B: Atomic and Molecular Physics* **7** L364 URL http://stacks.iop.org/0022-3700/7/i=12/a=003

[35] Burgess A and Tully J A 1992 *Astron. Astrophys.* **254** 436–453 URL http://adsabs.harvard.edu/abs/1992A%26A...254..436B

[36] Summers H P 1994 *ADAS manual* JET Joint Undertaking

[37] Badnell N R, Girffin D C, Gorczyca T W and Pindzola M S 1993 *Phys. Rev. A* **48** R2519

[38] Fernández-Menchero L, Del Zanna G and Badnell N R 2015 *Astron. Astrophys.* **577** A95